A duplicated zone of polarizing activity in polydactylous mouse mutants

Hiroshi Masuya,[1] Tomoko Sagai,[1] Shigeharu Wakana,[2] Kazuo Moriwaki,[3] and Toshihiko Shiroishi[1,4]

[1]Mammalian Genetics Laboratory, National Institute of Genetics, Mishima, Japan; [2]Central Institute for Experimental Animals, Kawasaki, Japan; [3]The Graduate University for Advanced Studies, Kamiyamaguchi, Hayama, Japan

The positional signaling along the anteroposterior axis of the developing vertebrate limb is provided by the zone of polarizing activity (ZPA) located at the posterior margin. Recently, it was established that the *Sonic hedgehog* (*Shh*) mediates ZPA activity. Here we report that a new mouse mutant, *Recombination induced mutant 4* (*Rim4*), and two old mutants, *Hemimelic extra toes* (*Hx*) and *Extra toes* (*Xt*), exhibit mirror-image duplications of the skeletal pattern of the digits. In situ hybridization of the embryos of these mutants revealed ectopic expression of *Shh* and *fibroblast growth factor-4* (*Fgf-4*) genes at the anterior margin of limb buds. The new mutation, *Rim4*, was mapped to chromosome 6 with linkage to *HoxA* but segregated from *HoxA*. No linkage to other known polydactylous mutations was detected. In this mutant, ectopic expression of the *Hoxd-11* gene, thought to be downstream of ZPA, was also observed at the anterior margin of the limb buds. All results indicate the presence of an additional ZPA at the anterior margin of limb buds in these mutants. Thus, it appears that multiple endogenous genes regulate the spatial localization of the ZPA in the developing mouse limb bud.

[*Key Words*: Mouse mutant; limb morphogenesis; ZPA; *Shh*; *Fgf-4*; preaxial polydactyly]

Received April 4, 1995; revised version accepted June 2, 1995.

In the vertebrate tetrapod limbs, each skeletal element shows a sequential pattern along the anteroposterior and proximodistal axes. The pattern formation along the two axes is controlled by the two signaling centers. Signaling along the anteroposterior axis is provided from the zone of polarizing activity (ZPA) at the posterior margin of limb bud mesoderm. The grafting of ZPA to the anterior margin of the second limb bud induces additional digits in a mirror-image sequence along the anteroposterior axis (Saunders and Gasseling 1968; Tickle et al. 1975; Tickle 1981). The pattern along the proximodistal axis is controlled by the signaling from the apical ectodermal ridge (AER).

It is postulated that *Sonic hedgehog* (*Shh*), a homolog of the segment polarity gene *hedgehog* in *Drosophila*, mediates ZPA activity (Echelard et al. 1993; Riddle et al. 1993; Chang et al. 1994). Activity downstream of ZPA is thought to be performed by genes such as *Hoxd* and *bone morphogenic protein-2* (*Bmp-2*), which may direct positional specification during pattern formation in the limbs (Dollé et al. 1989; Izpisúa-Belmonte et al. 1991; Nohno et al. 1991; Morgan et al. 1992; Niswander et al. 1993; Francis et al. 1994). It is also known that some members of the fibroblast growht factor (FGF) family expressed in the AER can functionally replace the AER (Niswander et al. 1993; Fallon et al. 1994). It has been evident for a long time that ZPA stimulates signaling of the AER, whereas the posterior portion of the AER maintains a functional ZPA in the posterior mesoderm (Todt and Fallon 1987). Recently, it was established that there is a positive feedback loop operating between the ZPA and the posterior AER, and expression of *Shh* and fibroblast growth factor-4 (*Fgf-4*) is coordinately regulated by this positive feedback (Laufer et al. 1994; Niswander et al. 1994).

It has been reported that retinoic acid (RA) converts cells in the anterior region of limb buds to cells with ZPA activity and that application of a bead soaked in RA to the anterior margin of limb bud induces mirror-image duplication of the limb as is observed in grafting ZPA to the anterior region (Tickle et al. 1982; Noji et al. 1991; Wanek et al. 1991; Tamura et al. 1993). It was proposed that application of RA beads to the anterior limb bud induces ectopic expression of *Fgf-4* in the anterior ridge. Then, FGF-4 and RA coordinately elicit *Shh* expression at the anterior margin of the limb bud (Niswander et al. 1994).

On the other hand, the cells at the anterior margin of the limb bud acquire the ZPA activity under microdissociation conditions or in vivo removal of AER (Anderson et al. 1994). There is, however, very little information on which endogenous genes regulate the spatial and temporal specificity of the ZPA and are involved in this conversion of the cells at the anterior margin to acquire ectopic ZPA activity.

In vertebrate tetrapods, there are many congenital ab-

[4]Corresponding author.

normalities affecting the pattern formation of limbs. Preaxial polydactyly, which causes extra digits on the side of digit 1, is one of the major abnormalities. Hyperphalangy (triphalangeal thumb) is also a major abnormality of limb pattern formation in mammals. It mainly involves transformation of diphalangeal digit 1 to a triphalangeal digit. Preaxial polydactyly is often coupled with hyperphalangy and malformation of the tibia (Yujnovsky et al. 1974; Atasu 1976; Canun et al. 1984). It is also associated with duplication of digits in a mirror-image along the anteroposterior axis in some cases (Landauer 1956; Forsthoefel 1958; Forsthoefel 1962). The molecular mechanisms by which these abnormalities of preaxial polydactyly are induced is poorly understood.

Many mouse mutants with the phenotype of preaxial polydactyly have already been described and have been genetically mapped. In this study we present characterization of a new polydactylous mutant, Recombination induced mutant 4 (*Rim4*), and two old polydactylous mutants, *Hemimelic extra toes* and *Extra toes* (*Hx* and *Xt*, respectively) all of which exhibit preaxial polydactyly. The *Rim4* mutation arose spontaneously from an intra-major histocompatibility complex (MHC) recombinant established from crosses between a wild-type mouse-derived MHC congenic strain (Shiroishi et al. 1982) and standard MHC congenic strain B10. A (Shiroishi et al. 1987a,b) *Rim4* shows preaxial polydactyly, which is inherited dominantly.

The *Hx* mutation induces preaxial polydactyly and hyperphalangy in all four feet, and malformation of the radius and tibia. Homozygotes of *Hx* probably die early during embryogenesis (Green 1989). *Hx* has been mapped to the proximal region of chromosome 5 (Fig. 1C), where the *Shh* gene was recently mapped (Chang et al. 1994). This chromosomal region is homologous to a segment of the long arm of human chromosome 7, where the genes responsible for a congenital polysyndactyly and triphalangeal thumb were mapped (Heutink et al. 1994; Tsukurov et al. 1994).

Xt is a semidominant mutation mapped to chromosome 13 (Lyon et al. 1967; Lyon and Meredith 1969) (Fig. 1C). This mutation affects the *Gli-3* gene (Schimmang et al. 1992, 1993, 1994; Vortkamp et al. 1992), which is a mouse homolog of the *Drosophila* segment polarity gene *cubitus interruptus* (Orenic et al. 1990; Hui et al. 1994). One of the mutant alleles, Xt^{J}, was caused by deletion of a DNA segment including the coding region (Hui and Joyner 1993). The heterozygotes of Xt^{J} show preaxial polydactyly of the hind feet with duplication of digit 1 (thumb polydactyly). Homozygotes die in utero or at birth with multiple abnormalities. The late-stage embryo of the homozygote shows preaxial polydactyly and hyperphalangy in all four limbs. In humans, deficiency of the *GLI3* gene results in the Greig cephalopolysyndactyly syndrome (GCPS) affecting limb and craniofacial development (Vortkamp et al. 1991).

Here, we demonstrate that three mouse mutants, *Rim4*, *Hx* and Xt^{J}, exhibit mirror-image duplication of the limb skeleton. Furthermore, *Shh* and *Fgf-4* are ectopically expressed at the anterior margin of the limb bud of

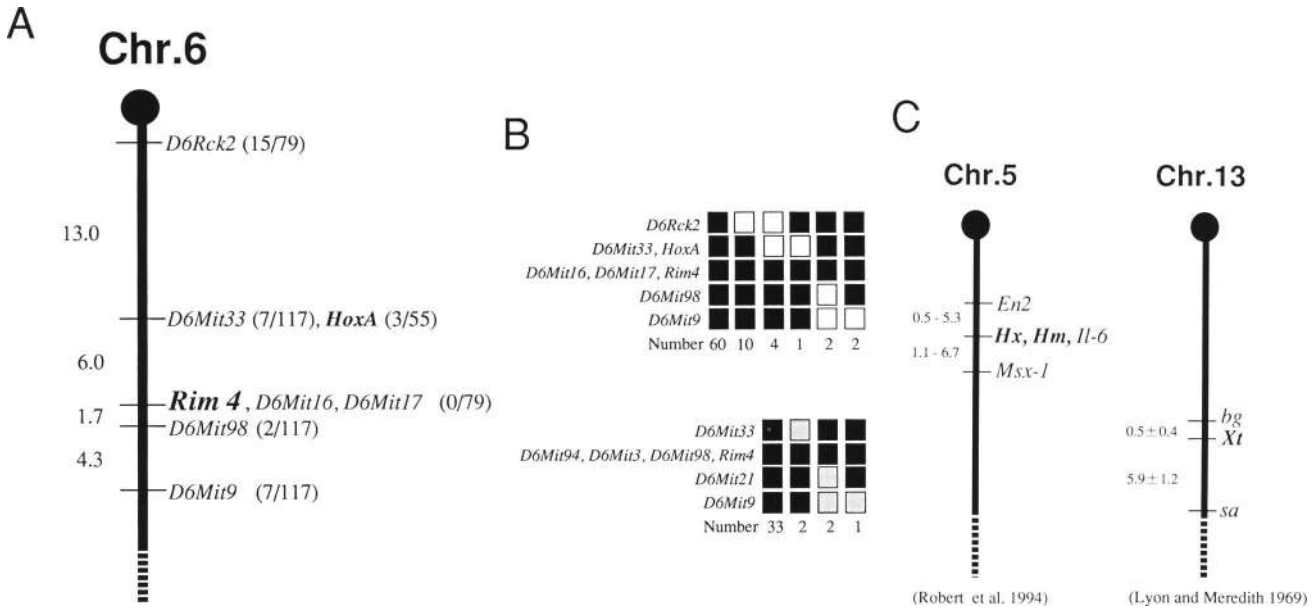

Figure 1. Genetic maps of three mouse mutants. (*A*) Mapping of *Rim4* to chromosome 6. The linkage data from the two backcrosses were compiled to construct the genetic map of *Rim4*. The number of recombinants between each marker and *Rim4* and the number of progeny screened are indicated in parentheses. (*B*) Segregation panels of cross 1 (C57BL/10J–*Rim4*/+ ×DBA/2J)F_1×C57BL/10J, and cross 2 (C57BL/10J–*Rim4*/+ ×NZB)F_1×C57BL/10J. The progeny from these two crosses were typed for loci listed at the *left* of each panel. The number of offspring inheriting each type of chromosome is listed at the *bottom* of each column. (Solid box) B10; (open box) DBA; (shaded box) NZB. (*C*) Chromosomal locations of *Hx* and *Xt* mutant genes in chromosomes 5 and 13, according to the gene mapping of *Hx* (Robert et al. 1994) and *Xt* (Lyon and Meredith 1969).

these mutants. On the basis of these findings, it appears that the additional ZPA is present in the anterior limb buds of these mutants. The results suggest that a major form of preaxial polydactylous mutations is caused by a duplicated ZPA at the anterior margin of the limb buds. Thus, these mutants should provide a clue to identify endogenous genes involved in regulation of the spatial localization of ZPA in limb development.

Results

Genetic mapping of Rim4

To determine the chromosomal location of the *Rim4* gene and to analyze potential linkage with other mouse polydactylous mutants and other known genes, we carried out linkage analysis of *Rim4* in crosses with two laboratory strains, DBA/2J and NZB. Because the penetrance of *Rim4* was incomplete, we used only the backcross progeny, which showed polydactyly. As a result, *Rim4* was mapped to chromosome 6 and found to be tightly linked to *HoxA*, *D6Mit16*, and *D6Mit17* (Fig. 1A). The *Hoxa* gene cluster is involved in limb development and has been mapped closely to *cbl-1* (Moore et al. 1992).

In the present linkage analysis, *HoxA* was tightly linked to *D6Mit33*, and three recombinants were obtained between *HoxA* and *Rim4*, indicating that *Rim4* is separate from *HoxA* (Fig. 1). In the proximal region of chromosome 6, the *hop-sterile* (*hop*) mutation, which is associated with preaxial polydactyly of both fore- and hindfeet, was mapped between *sightless* (*Sig*) and *Hypodactyly* (*Hd*) loci in the following gene order from proximal to distal; *Sig*–(15.8±1.7 cM)–*hop*–(9.6±1.5 cM)–*Hd* (Hollander 1976). *Hd* was mapped to 1.5 cM proximal to *Hoxa3* (Mock et al. 1987), indicating that the *Rim4* gene is distinct from the *hop* gene and located at a distance of 15 cM from *hop*. Because the position of *Rim4* does not overlap with the other mutant loci associated with polydactyly, *Rim4* appears to be a novel mutation at a new locus that affects limb pattern formation.

Skeletal phenotypes of Rim4*; homozygotes and heterozygotes*

On the basis of the genotyping with the microsatellite marker loci that are linked to *Rim4*, we were able to distinguish homozygotes from heterozygotes. The genotypes of progeny obtained from intercross of F_1 mice between C57BL/10–*Rim4*/+ stock and the NZB strain were determined with appropriate microsatellite markers. A typical phenotype of *Rim4* heterozygotes is a triphalangeal extra digit located on the preaxial side of digit 1 of the hindlimbs (Fig. 2B,E). Duplication of the digit in the heterozygotes varied from thickening of diphalangeal digit 1 to branching of triphalangeal extra digits, which resulted in a total of seven toes. The digit duplication was restricted in autopods of the hindlimbs.

In the homozygotes, the affected domain was enlarged to more proximal elements than heterozygotes, namely zeugopods and autopods. The forelimbs were also affected, but the penetrance was incomplete and the polydactyly was less extreme than that of the hindlimbs. The affected domain was restricted in autopods in the forelimbs. In most cases, the distal portion of the tibia was reduced in length and the ankle joint was disturbed (Fig. 3F). Digit 1 was lost and there were two or more triphalangeal extra digits. The digits of the mouse, except for digit 1, did not appear to be as distinct. Because the second and third tarsal bones were duplicated in mirror image (Fig. 2C,F), the digit pattern of *Rim4* homozygotes was concluded to be (IV-)III-II-II-III-IV-V. Variations in affected tibia ranged from only shortening or thinning of the distal end of the tibia to complete absence of the tibia. The total number of digits on a limb varied from five to seven. With respect to the axial structure, transformation of the presacral vertebrae to sacrum was often observed in homozygotes (data not shown). Many variants of the phenotype were found in both heterozygotes and homozygotes with the same genetic background, and the right and left limbs were affected independently.

The defect in the limb skeleton of *Rim4* homozygotes resembles those of homozygotes of *luxate* (*lx*) mapped to chromosome 5 (Carter 1951), heterozygotes of *Hx* mapped to chromosome 5 (Knundsen and Kochhar 1981), and hetero- and hemizygotes of *X-linked polydactyly* (*Xpl*) mapped to chromosome X (Sweet and Lane 1980). The skeletal phenotype of *lx* in particular resembles that of *Rim4* in both heterozygotes and homozygotes (Carter 1951). Abnormalities of the kidney, reported in *lx* or *Xpl* mice (Carter 1954; Sweet and Lane 1980) were not observed.

To ascertain when the polydactyly of *Rim4* occurred in the developmental stages, we characterized the skeletal phenotype of *Rim4* embryos according to the developmental stages. In the embryos of *Rim4* homozygotes, there were individuals with phenotypes that were much more severe than those observed in adult mice. In the most extreme case, a fibula-like element was formed on the anterior side and the calcaneus was duplicated (Fig. 3D,F). The polydactyly could be already recognized at the initial stage of condensation of cartilage when outgrowth had been induced ectopically in the anterior portion of the limb bud at 13 days [stage 7 of the staging system for mouse limb development (Fig. 3B; Wanek et al. 1989)].

Duplicated ZPA in Rim4

To examine whether the mirror-image duplication is caused by ectopic ZPA activity at the anterior region of the limb buds, we carried out whole-mount in situ hybridization of *Rim4* embryos using riboprobes of the *Shh*, *Fgf-4*, and *hoxd11* genes. The genotypes of the embryos from intercrosses of F_1 mice between C57BL/10–*Rim4*/+ stock and NZB strain were identified by microsatellite DNA markers, as was done in characterization of the skeletal phenotype.

In the wild-type embryos, *Shh* was expressed in the mesoderm exclusively at the posterior margin of both the fore- and hindlimbs from stage 1 of limb develop-

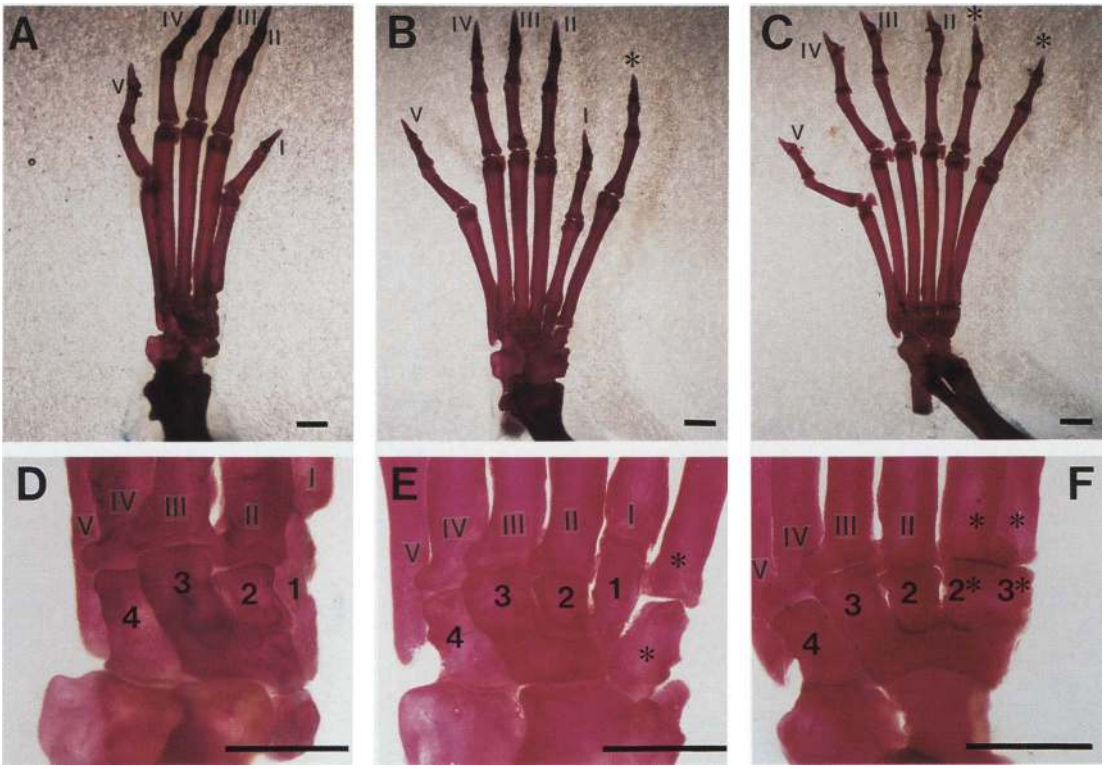

Figure 2. Skeletal phenotypes of the hindlimbs of *Rim4* mice. Dorsal view of the hindlimbs stained with alcian blue and alizarin red. Wild-type digits are numbered I–V from anterior to posterior, and the first to fourth tarsal bones are numbered 1–4. Duplicated digits are indicated by asterisks. (*A–F*) Left hindlimbs of adult mice. (*D–F*) Magnifications of feet shown in *A–C*. (*A,D*) Wild-type foot plate of a mouse obtained from the backcross NZB×(NZB×C57BL/10–*Rim4*/+) F_1. (*B,E*) Typical phenotype of the foot plate of a *Rim4* heterozygote, C57BL/10J–*Rim4*/+. (*C,F*) Typical phenotype of the foot plate of a *Rim4* homozygote obtained from the intercross of (NZB×C57BL/10–*Rim4*/+)F_1. (*F*) Second and third tarsal bones of the homozygotes were duplicated in a mirror image. Bars, 1.0 mm.

ment (10 days for the hindlimb) to stage 7 (13 days for the hindlimb). *Fgf-4* was expressed in the central–posterior portion of AER from stages 1 to 7. The expression domain of *Fgf-4* overlays in part that of *Shh* at the posterior limb bud. In stage 5 (12 days for hindlimb) the expression of *hoxd11* spread over the posterior and distal regions (Fig. 4).

In homozygotes of *Rim4*, *Shh* and *Fgf-4* were expressed ectopically at the anterior portion of the hindlimbs from stage 3 (11 days for the hindlimb) to stage 7 (Fig. 4). Ectopic expression of *Shh* was restricted to a relatively small region when compared with the normal expression at the posterior margin. The domain of ectopic expression of *Fgf-4* gene might be small as well. Endogenous and ectopic expression domain of *Fgf-4* might join at the anterior boundary of the endogenous expression, leading to the prolonged expression domain of *Fgf-4* (Fig. 4H). The ectopic expression of *Shh* and *Fgf-4* was prominent in stage 5 or 6 (12 days for the hindlimb and 11 days for the forelimb), in contrast to endogenous expression in the stage 3 or 4 (11 days for the hindlimb and 10 days for the forelimb). *Hoxd11* was expressed in both the anterior and posterior regions (Fig. 4D).

The ectopic expression of the *Shh*, *Fgf-4*, and the *hoxd11* genes at the anterior part of the limb, as well as the mirror-image duplication of the skeletal pattern, indicated that there was an additional ZPA located at the anterior margin of the hindlimb buds of the *Rim4* embryos. Ectopic outgrowth of this region was observed in sequential stages (Fig. 4D,F).

In the heterozygotes, the phenotype of the hindlimbs was less extreme than that of homozygotes, but ectopic expression of *Shh* and *Fgf-4* was also observed. The expression domains of these genes in the heterozygotes were narrower than those of the homozygotes, being restricted to the pinpoint regions at the anterior margin of the limb buds (data not shown).

Duplicated ZPA in two old polydactylous mutants

We also carried out characterization of skeletal phenotypes and whole-mount in situ hybridization of embryos of two other mutants, *Hx* and *Xt*, which show preaxial polydactyly similar to *Rim4*, using probes of the *Shh* and *Fgf-4* genes.

The embryos were obtained from the backcross of *Hx* heterozygotes to wild-type C57BL10 mice. The heterozygotes of *Hx* show preaxial polydactyly and hyperphalangy in all four feet, and malformation of the radius and tibia (Knundsen and Kochhar 1981). Skeletal phenotypes

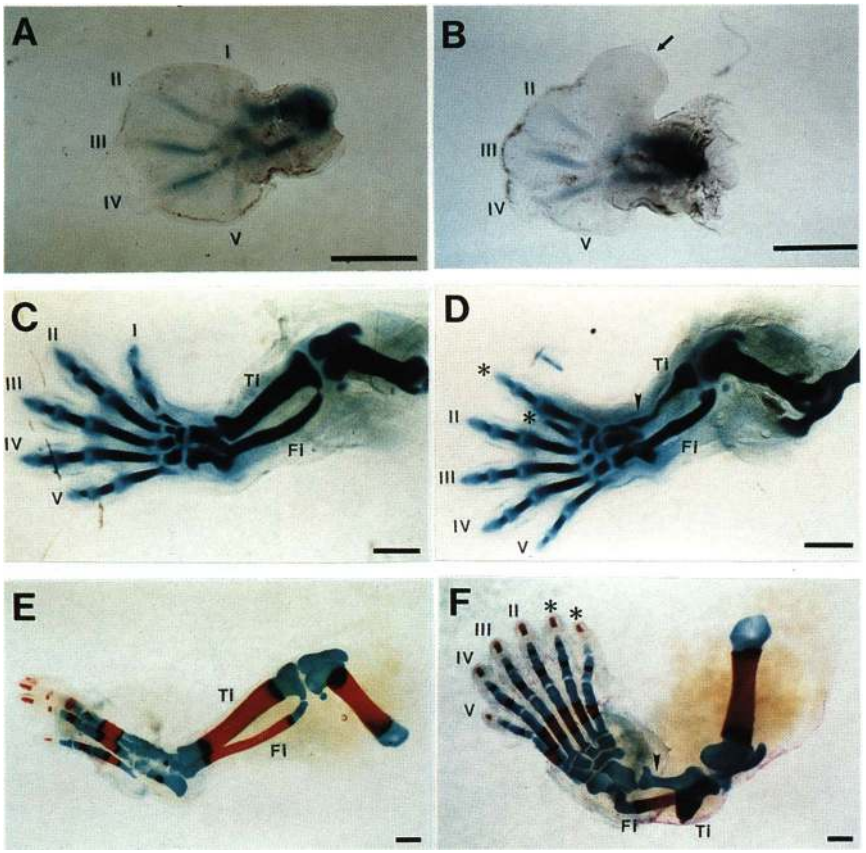

Figure 3. Skeletal phenotypes of *Rim4* embryos in various developmental stages. Dorsal view of the hindlimbs stained with alcian blue and alizarin red. (*A,C,E*) Skeletons of the wild-type embryos; (*B,D,F*) the skeletons of *Rim4* homozygotes. (*A,B*) 13.5-day (stage 8) embryo; (*C,D*) 15.5-day (stage 11) embryo; (*E,F*) 19.5-day (stage 13) embryo. (*B*) The arrow indicates the outgrowth at the anterior margin of the hindlimb bud of a *Rim4* homozygote. (*D,F*)Arrowheads indicate a fibula-like element formed on the anterior side of a reduced tibia. (*D*)Calcaneus was duplicated. Wild-type digits are numbered in the same way as in Fig. 1. Bars, 1.0 mm.

of the hindlimb of the *Hx* heterozygotes resemble the *Rim4* homozygotes with a III-II-II-III-IV-V digit pattern and mirror-image duplication of the second and third tarsal bones. They differ from *Rim4* in that the autopods of the forelimbs and hindlimbs are equally affected. Of nine embryos examined, five ectopically expressed *Shh* and *Fgf-4* at anterior margin of fore- and hindlimb buds at stage 6 (Fig. 5C,E). Ectopic expression of *Shh* spread more widely than that of *Rim4* homozygotes (data not shown).

The embryos were obtained from intercross of Xt^J heterozygotes. The heterozygotes showed duplication of digit 1 (thumb polydactyly) of the hindlimbs, which was less extreme than the phenotype of *Rim4* heterozygotes. The late-stage embryos of the homozygotes showed mirror-image duplication of digits in all four limbs and reduction of the tibia as was seen in *Rim4* homozygotes (Fig. 5B). We found that 1 of the 10 embryos expressed *Shh* ectopically at the anterior mesoderm of all four limb buds. Ectopic expression of *Fgf-4* was also observed in one embryo in the anterior AER in stage 5 (Fig. 5D,F).

Discussion

Preaxial polydactyly and duplication of ZPA

Preaxial polydactyly with hyperphalangy and malformation of the tibia represents a major group of congenital abnormalities of limbs in mice. In this study we showed that three polydactylous mouse mutations, *Rim4*, *Hx* and *Xt*, exhibit mirror-image duplication of the anterior–distal part of the limbs, which was caused by duplication of the ZPA at the anterior margin of the limb bud. The skeleton of the autopod of these mutants showed complete or slightly disturbed mirror-image duplication. In the same way, more proximal elements such as the fibula were sometimes duplicated in a mirror image. In many cases, however, the tibia was reduced in length, and in the most severe case, it was completely absent. In *Hx* heterozygotes, it was reported that this reduction of the tibia is caused by necrosis of presumptive tibial chondroblasts (Knundsen and Kochhar 1981). This necrosis may result from the disruption of the positional value of the region where the tibia is formed in limb development, which is caused by ectopic positional signaling from duplicated ZPA.

In mice, other polydactylous mutants, such as *luxoid* (*lu*), *Strong's luxoid* (*lst*), *lx*, and *Xpl*, also show mirror-image duplication of digits along the anteroposterior axis (Carter 1951, 1954; Forsthoefel 1958, 1962; Sweet and Lane 1980). In humans congenital preaxial polydactyly has been classified into four types: (1) thumb polydactyly, (2) polydactyly of the triphalangeal thumb, (3) polydactyly of the index finger, and (4) polysyndactyly (McKusick 1990). They can be regarded as morphogenic abnormalities along the anteroposterior axis of limb development. Preaxial polydactyly with hyperphalangy is a major group among these abnormalities, in which

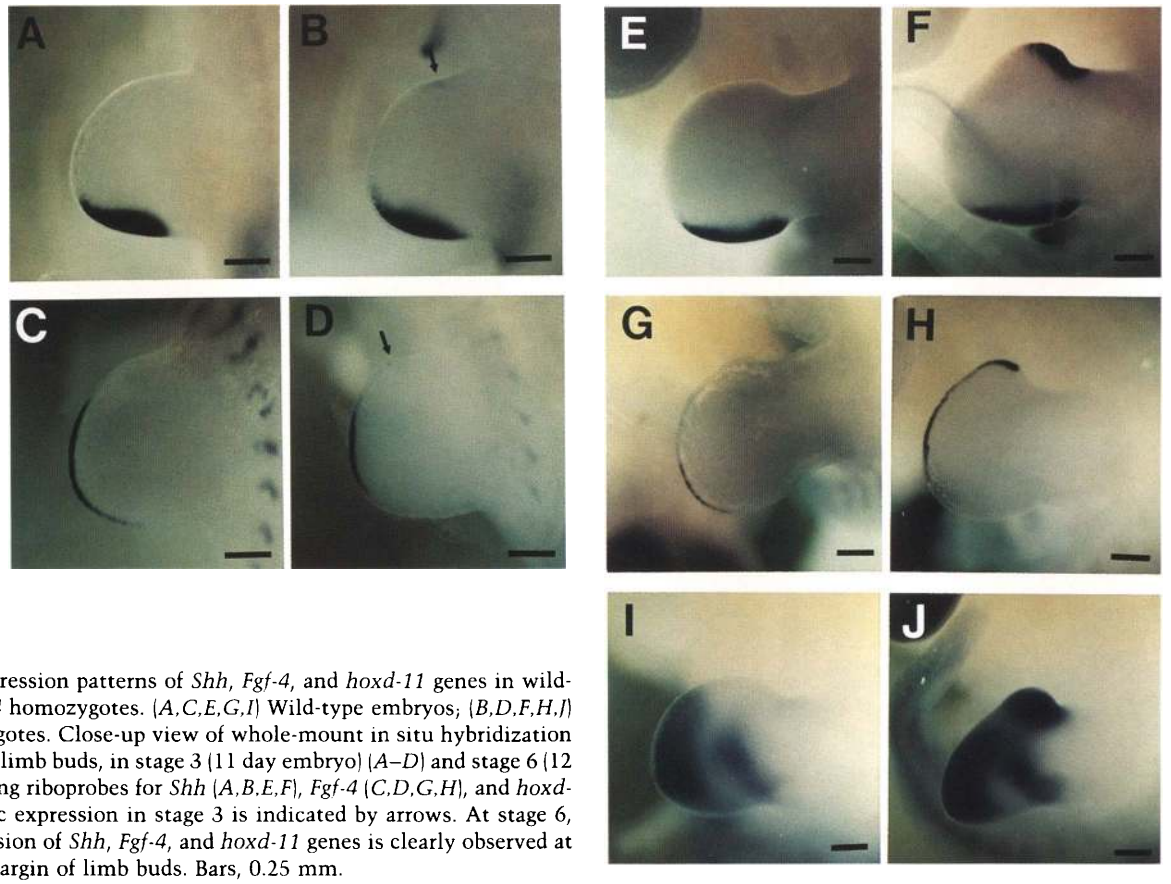

Figure 4. Expression patterns of *Shh*, *Fgf-4*, and *hoxd-11* genes in wild-type and *Rim4* homozygotes. (*A,C,E,G,I*) Wild-type embryos; (*B,D,F,H,J*) *Rim4* homozygotes. Close-up view of whole-mount in situ hybridization of the left hindlimb buds, in stage 3 (11 day embryo) (*A–D*) and stage 6 (12 days) (*E–J*), using riboprobes for *Shh* (*A,B,E,F*), *Fgf-4* (*C,D,G,H*), and *hoxd-11* (*I,J*). Ectopic expression in stage 3 is indicated by arrows. At stage 6, ectopic expression of *Shh*, *Fgf-4*, and *hoxd-11* genes is clearly observed at the anterior margin of limb buds. Bars, 0.25 mm.

hypoplasia or duplication of the tibia and radius is present in some cases. Their pattern of digits appears to be mirror-image duplication (Yujnovsky et al. 1974; Canun et al. 1984). Our results from this study suggest that most of this congenital polydactyly can be caused by duplication of ZPA at the anterior margin of the limb bud.

Temporal expression pattern of Shh *and* Fgf-4 *genes in* Rim4

In the *Rim4* mutant, the first ectopic expressions of *Shh* and *Fgf-4* genes were detected at the same time, in stage 3. This is different from RA application, in which ectopic expression of *Fgf-4* precedes that of *Shh*. In the earlier stage, the ectopic expression of *Shh* and *Fgf-4* could not be detected in *Rim4*. At stage 3, the domains of ectopic expression of *Shh* and *Fgf-4* were restricted in the pinpoint region at the anterior margin of limb buds. The *Rim4* mutation may induce ectopic ZPA in a small region. Once ectopic ZPA is induced, a positive feedback loop between ZPA and AER may enlarge both ectopic ZPA and posteriorized AER at the anterior limb bud.

Genetic regulation localizing ZPA to the posterior limb bud

It was reported recently that ectopic expression of the *Hoxb-8* transgene caused posterior homeotic transformation of axial structures (Charité et al. 1994). In addition, mirror-image duplication of the digits of the forelimbs accompanied by ectopic expression of the *Shh* and *Fgf-4* gene at the anterior margin of the limb buds was observed in transgenic mice. This phenotype is very similar to those in mouse mutants *Rim4*, *Hx*, and *Xt*, in that ectopic ZPA was observed at the anterior margin of limb buds.

It is clear that the regulation polarizing ZPA only at the posterior margin of limb buds was affected in the mutations that occurred in *Hoxb-8* transgenic mouse. At least three possibilities explain the cause of polydactyly appearing in these mutants. First, the mutations affect the regulatory region of the *Shh* gene, which results in induction of ectopic *Shh* expression at the anterior margin of the limb bud in addition to normal expression. Recently, the mouse *Shh* gene, *Hhg-1*, was mapped to the proximal region of chromosome 5 where *Hx* had been mapped (Chang et al. 1994). It is possible that the *Hx* mutation alters the spatial pattern of the expression of the *Shh* gene so that it is expressed ectopically at the anterior margin of the limb bud. Fine linkage analysis between *Hhg-1* and *Hx*, and molecular characterization of the *Hhg-1* gene from *Hx* mutant would address this possibility.

Second, as was shown in *Hoxb-8* transgenic mice, it is likely that ectopic expression of some member of *Hox* gene clusters may elicit a duplicated ZPA at the anterior margin of the limb bud. From the data of genetic linkage of the three mutations *Rim4*, *Hx*, and *Xt*, none of them

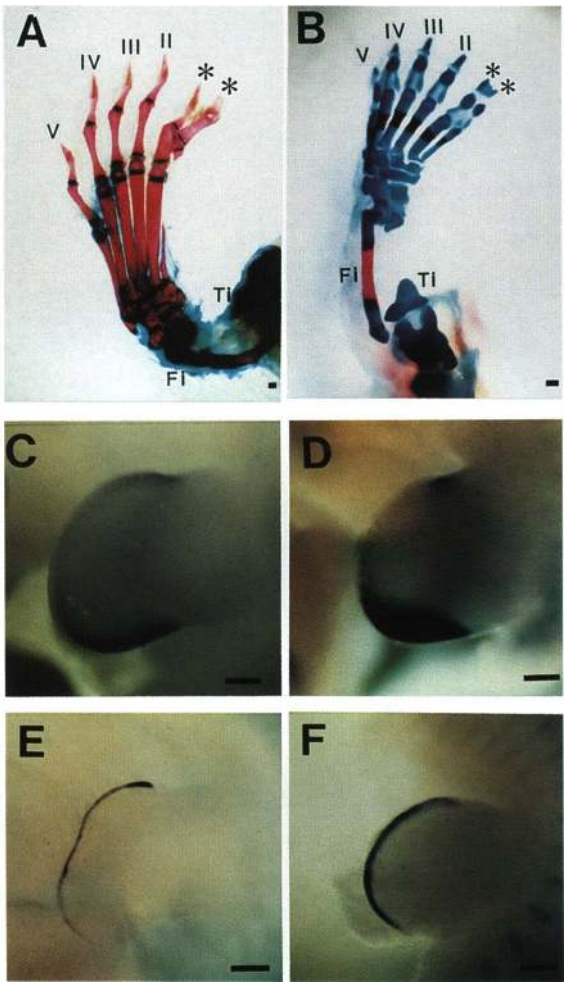

Figure 5. Mirror-image duplication and ectopic expression of *Shh* and *Fgf-4* in *Hx* and *Xt*. (*A*,*C*,*E*) *Hx* heterozygotes; (*B*,*D*,*F*) *Xt* homozygotes. Dorsal view of the left hindlimbs of adults stained with alcian blue and alizarin red (*A*,*B*), and whole-mount in situ hybridization of the embryos (*C*–*F*) at stage 5 or 6 (12-day embryo), using riboprobes for *Shh* (*C*,*D*) and *Fgf-4* (*E*,*F*). Wild-type digits are numbered in the same way as in Fig. 1. Bars, 0.25 mm.

appears to be closely linked with the *Hox* gene clusters. Therefore, the possibility that the mutations occur in the *Hox* gene clusters per se can be excluded.

The third possibility is that the wild-type genes of the mutant loci down-regulate ZPA activity in a region-specific manner. The mutations might affect the region-specific suppression of ZPA activity and induce ectopic expression of ZPA at the anterior margin of limb buds, finally leading to bilateral ZPA in limb buds. It was reported that cells in anterior limb buds possess potential ZPA activity when they are cultured under microdissociation conditions or in vivo removal of the AER (Anderson et al. 1994). Such potential ZPA activity at the anterior margin must be suppressed in normal limb development under the anterior part of the AER. The wild-type alleles of *Rim4*, *Hx*, and *Xt* loci might be involved in a cascade of down-regulation of the activity of ZPA specifically at the anterior margins of the limb buds. In this context, it is of interest to note that the Xt^J mutation has a deletion including the zinc finger domain of the *Gli-3* gene which encodes a transcription factor, resulting in loss of function of this gene. This suggests the existence of a genetic pathway that suppresses the ZPA activity specifically at the anterior margin of the limb bud in normal mouse embryos.

As stated above, there are many other polydactylous mutants that exhibit hyperphalangy and malformation of the tibia, whose phenotypes resemble those of *Rim4*, *Hx*, and *Xt* (Carter 1951, 1954; Forsthoefel 1958, 1962). In some cases, mirror-image duplication of digits is observed. This study suggests that many other genes may have functions to down-regulate ZPA activity at the anterior margin of limb buds.

Materials and methods

Mice

Multiple visible mutants arose spontaneously from intra-MHC recombinants established from crosses between a wild-type mouse-derived MHC congenic strain, B10.MOL-SGR (Shiroishi et al. 1982) and standard MHC congenic strain B10. A (Shiroishi et al. 1987a,b). They were designated recombination-induced mutants (*Rim*; T. Shiroishi, T. Sagai, M. Yoshino, H. Masuya, M. Maeda, S. Wakana, and K. Moriwaki, in prep.). One of them, *Rim4*, exhibits preaxial polydactyly of the hind feet and occasional malformation of the tibia. The mutant was backcrossed to the C57BL/10 strain and the mutant gene was maintained in this genetic background.

Hx mice, B10.D2/nSn–*Hx*/+, were purchased from the Jackson Laboratory. To maintain the *Hx* mutant gene, the heterozygotes were backcrossed to the wild-type, B10.D2/nSn–+/+, mice. For whole-mount in situ hybridization, embryos were obtained from the crossing of *Hx* male mice and C57BL/10 female mice.

Xt mice, C3HeB/FeJ–E^{so}/E^{so} Xt^J/+, were purchased from the Jackson Laboratory. To maintain the *Xt* mutant gene, the heterozygotes were intercrossed. For whole-mount in situ hybridization, embryos were obtained from the intercrossing of the heterozygotes.

Linkage analysis

Linkage analysis was carried out using two types of backcrosses: (C57BL/10–*Rim4*/+×DBA/2J)F_1 and (C57BL/10–*Rim4*/+×NZB)F_1 were backcrossed to C57BL/10J. They were designated backcrosses 1 and 2, respectively. In the analysis, the penetrance of *Rim4* was incomplete. In backcross 1, the penetrance was 71.1%, and in backcross 2, it was 92.8%. Seventy-nine and 38 offspring that exhibited polydactyly from backcrosses 1 and 2, respectively, were used in the linkage analysis. Genomic DNA was prepared from the liver or tail of the backcrossed progeny. The microsatellite marker loci were typed by simple sequence length polymorphism (SSLP) according to the protocol of Research Genetics (Huntsville, AL). The *Hoxa* gene was typed by Southern analysis using a 3.7-kb genomic DNA probe that contains the 3′ end of the *Hoxa-6* gene and the 5′ end of the *Hoxa-5* gene (Odenwald et al. 1987; Fibi et al. 1988). Digestion with *Hin*fI gave RFLP fragments of 0.15 kb for C57BL/10J and 0.2 kb for DBA/2J. The linkage data from these two crosses were compiled to construct the genetic map of *Rim4*.

Genotyping of Rim4 *mice*

For analysis of the *Rim4* phenotype, the progeny obtained from the intercross of (NZB×C57BL/10–*Rim4*/+)F_1 was genotyped. Genomic DNA was prepared from the liver of the adult mice or the head of the embryos after whole-mount in situ hybridization. The genotype of the progeny was determined by reference to microsatellite markers *D6Mit9*, *D6Mit33*, and *D6Mit98*.

Skeletal preparations

Double staining of the skeleton with alcian blue and alizarin red was performed essentially as described elsewhere (Wallin et al. 1994).

In situ hybridization

Whole-mount in situ hybridization using digoxygenin-labeled RNA was performed essentially as described elsewhere (Wilkinson 1992). For the detection of weak expression, color reaction using X-phosphate and NBT was performed for a total of 6 hr (1.5 hr×4 reactions). The probe for *Shh* was transcribed from a 642-bp *Eco*RI fragment by T3 polymerase (Echelard et al. 1993), and the probe for *Fgf-4* was transcribed from a 620-bp fragment by T3 polymerase (Niswander et al. 1992). The *hoxd11* probe was a 300-bp transcript generated by T7 polymerase (Izpisúa-Belmonte et al. 1991).

Acknowledgments

We are grateful to Drs. D. Duboule, A. McMahon, G. R. Martin, and N. Takahashi for making available the *hoxd-11*, *Shh*, *Fgf-4*, and *Hoxa-5-Hoxa-6* probes, to Drs. E. Kawase, Y. Shirayosi, and N. Nakatsuji for technical advice regarding whole-mount in situ hybridization, to Dr. H. Koseki for technical advice regarding staining of the skeleton, and to Drs. H. Ide and K. Tamura for reading the manuscript and giving useful comments and discussion. This study was supported in part by grants-in-aid from the Ministry of Education, Science and Culture of Japan. This work is contribution no. 2022 from the National Institute of Genetics, Japan.

The publication costs of this article were defrayed in part by payment of page charges. This article must therefore be hereby marked "advertisement" in accordance with 18 USC section 1734 solely to indicate this fact.

References

Anderson, R., M. Landry, A. Reginelli, G. Taylor, C. Achikar, L. Gudas, and K. Muneoka. 1994. Conversion of anterior limb bud cells to ZPA signaling cells in vitro and in vivo. *Dev. Biol.* **164:** 241–257.

Atasu, M. 1976. Hereditary index finger polydactyly: Phenotypic, radiological, dermatoglyphic, and genetic findings in a large family. *J. Med. Genet.* **13:** 469–476.

Canun, S., R.M. Lomeli, R. Martinez, and A. Carnevale. 1984. Absent tibiae, triphalangeal thumbs and polydactyly: Description of a family and prenatal diagnosis. *Clin. Genet.* **25:** 182–186.

Carter, T.C. 1951. The genetics of luxate mice. I. Morphological abnormalities of heterozygotes and homozygotes. *J. Genet.* **50:** 441–457.

———. 1954. The genetics of luxate mice. IV. Embryology. *J. Genet.* **52:** 1–35.

Chang, D.T., A. Lopez, D.P. Kessler, C. Chang, B.K. Simandl, R. Zhao, M.F. Seldin, J.F. Fallon, and A.P. Beachy. 1994. Products, genetic linkage and limb patterning activity of a murine *hedgehog* gene. *Development* **120:** 3339–3353.

Charité, J., W. Guaaff, S. Shen, and J. Deschamps. 1994. Ectopic expression of Hoxb-8 causes duplication of the ZPA in the forelimb and homeotic transformation of axial structures. *Cell* **78:** 589–601.

Dollé, P., J.-C. Izpisúa-Belmonte, H. Falkenstein, A. Renucci, and D. Duboule. 1989. Codinate expression of murine Hox5 complex homeobox-containing genes during limb pattern formation. *Nature* **342:** 767–722.

Echelard, Y., D.J. Epstein, B. St-Jacques, L. Shen, J. Mohler, J.A. McMahon, and A. McMahon. 1993. Sonic hedgehog, a member of a family of putative signaling molecules, is implicated in the regulation of CNS polarity. *Cell* **75:** 1417–1430.

Fallon, J.F., A. Lopez, M.A. Ros, M.P. Savage, B.B. Olwin, and B.K. Simandl. 1994. FGF-2: Apical ectodermal ridge growth signal for chick limb development. *Science* **264:** 104–107.

Fibi, M., B. Zink, M. Kessel, A.M. Colber-Poley, S. Labeit, H. Learch, and P. Guruss. 1988. Coding sequence and expression of the homeobox gene Hox 1.3. *Development* **102:** 349–359.

Forsthoefel, P.F. 1958. The skeletal effects of the luxoid gene in mouse, including its interaction with the luxate gene. *J. Morphol.* **102:** 247–287.

———. 1962. Genetics and manifold effects of Strong's luxoid gene in mouse, including its interactions with Green's luxoid and Carter's luxate genes. *J. Morphol.* **110:** 391–420.

Francis, P.H., M.K. Richardson, P.M. Brickell, and C. Tickle. 1994. Bone morphogenetic proteins and a signaling pathway that controls patterning in the developing chick limb. *Development* **120:** 209–218.

Green, M.C. 1989. Catalog of mutant genes and polymorphic loci. In *Genetic variants and strains of the laboratory mouse* (ed. M. F. Lyon and A. G. Searle), vol. pp. Oxford University Press, Oxford, UK.

Heutink, P., J. Zguricas, L. van Oosterhout, G.J. Breedveld, L. Testers, L.A. Sandkuijl, P.J.L.M. Snijders, J. Weissenbach, D. Lindhout, S.E.R. Hovius, and B.A. Oostra. 1994. The gene for triphalangeal thumb maps to the subtelomellic region of chromosome 7q. *Nature Genet.* **6:** 287–292.

Hollander, W.F. 1976. Hydrocephalic polydactyly, a recessive pleiotropic mutant in the mouse, and its location in chromosome 6. *Iowa State J. Res.* **51:** 13–23.

Hui, C.C. and A.L. Joyner. 1993. A mouse model of Greig cephalopolysyndactyly syndrome: The extra-toes^J mutation contains an intragenic deletion of the Gli3 gene. *Nature Genet.* **3:** 241–246.

Hui, C.C., D. Slusarski, K.A. Platt, R. Holmgren, and A.L. Joyner. 1994. Expression of three mouse homologs of the Drosophila segment polarity gene cubitus interruptus, Gli, Gli-2, and Gli-3, in ectoderm- and mesoderm-derived tissues suggests multiple roles during postimplantation development. *Dev. Biol.* **162:** 402–413.

Izpisúa-Belmonte, J.-C., C. Tickle, P. Dolle, L. Wolpert, and D. Duboule. 1991. Expression of the homeobox Hox-4 genes and specification of position in chick wing development. *Nature* **350:** 585–589.

Knundsen, T.B. and D.M. Kochhar. 1981. The role of morphogenetic cell death during abnormal limb bud out growth in mice heterozygous for the dominant mutation Hemimelic-extra toe (Hm^x). *J. Embryol. Exp. Morphol.* (Suppl.) **65:** 289–307.

Landauer, W. 1956. Rudimentation and duplication of the radius in the duplicate mutant form of fowl. *J. Genet.* **54:** 199–218.

Laufer, E., C.E. Nelson, R.L. Johnson, B.A. Morgan, and C. Tabin. 1994. Sonic hedgehog and Fgf-4 act through a signaling cascade and feedback loop to integrate growth and pat-

terning of the developing limb bud. *Cell* **79:** 993–1003.

Lyon, M.F. and R. Meredith. 1969. Muted, a new mutant affecting coat color and otoliths of the mouse, and its position in linkage group XIV. *Genet. Res.* **14:** 163–166.

Lyon, M.F., T. Morris, A.G. Searle, and J. Butler. 1967. Occurrences and linkage relations of the mutant "extra-toes" in the mouse. *Genet. Res.* **9:** 383–385.

McKusick, V.A. 1990. Autosomal dominant phenotypes. In *Mendelian inheritance in man: Catalogs of autosomal dominant, autosomal recessive, and X-linked phenotypes* (ed. V. A. McKusick),vol. 9 pp. 765–766. The Johns Hopkins University Press, Baltimore, MD.

Mock, B.A., L.A. D'Hoostelaere, R. Matthai, and K. Huppi. 1987. A mouse homeobox gene, Hox-1.5, and the morphological locus, *Hd*, map to within 1 cM on chromosome 6. *Genetics* **116:** 607–612.

Moore, K.J., M.A. D'Amore Bruno, T.R. Korfhagen, S.W. Glasser, J.A. Whitsett, N.A. Jenkins, and N.G. Copeland. 1992. Chromosomal localization of three pulmonary surfactant protein genes in the mouse. *Genomics* **12:** 388–393.

Morgan, B.A., J.C. Izpisúa-Belmonte, D. Duboule, and C. J. Tabin. 1992. Targeted misexpression of Hox-4.6 in avian limb bud causes apparent homeotic transformations. *Nature* **358:** 236–239.

Niswander, L. and G.R. Martin. 1992. Fgf-4 expression during gastrulation, myogenesis, limb and tooth development in the mouse. *Development* **114:** 755–768.

———. 1993. FGF-4 and BMP-2 have opposite effects on limb growth. *Nature* **361:** 68–71.

Niswander, L., C. Tickle, A. Vogel, I. Booth, and G.R. Martin. 1993. FGF-4 replaces the apical ectodermal ridge and directs outgrowth and patterning of the limb. *Cell* **75:** 579–587.

Niswander, N., S. Jeffley, G.R. Martin, and C. Tickle. 1994. A positive feedback loop coodinates growth and patterning in the vertebrate limb. *Nature* **371:** 609–612.

Nohno, T., S. Noji, E. Koyama, K. Ohyama, F. Myokai, A. Kuroiwa, T. Saito, and S. Taniguchi. 1991. Involvement of the Chox-4 chicken homeobox genes in determination of anteroposterior axial polarity during limb development. *Cell* **64:** 1197–1205.

Noji, S., T. Nohno, E. Koyama, K. Muto, K. Ohyama, Y. Aoki, K. Tamura, K. Ohsugi, H. Ide, S. Taniguchi, and T. Saito. 1991. Retinoic acid induces polarizing activity but is unlikely to be a morphogen in the chick limb bud. *Nature* **350:** 80–86.

Odenwald, W.F., C.F. Taylor, F.J. Palmer-Hill, J.V. Friedrich, M. Tani, and R. A. Lazzarini. 1987. Expression of a homeo domain protein in noncontact-inhibited cultured cells and postmitotic neurons. *Genes & Dev.* **1:** 482–496.

Orenic, T.V., D.C. Slusarski, K.L. Kroll, and R.A. Holmgren. 1990. Cloning and characterization of the segment polarity gene *cubitus interruptus* Dominant of *Drosophila*. *Genes & Dev.* **4:** 1053–1067.

Riddle, R.D., R.L. Johnson, E. Laufer, and C. Tabin. 1993. Sonic Hedgehog mediates the polarizing activity of ZPA. *Cell* **75:** 1401–1416.

Robert, B., X. Montagutelli, D. Houzelstein, L. Ferland, A. Cohen, M. Buckingham, and J.-L. Guénet. 1994. Msx1 is close but not allelic to either Hm or Hx on mouse chromosome 5. *Mamm. Genome* **5:** 446–449.

Saunders, J.W. and M.T. Gasseling. 1968. Ectodermal-mesenchymal interactions in the origin of limb symmetry. In *Epithelial-mesenchymal interactions* (ed. R. Fleischmajor and R. E. Billingham), pp. 78–97. Wiliams & Wilkins, Baltimore, MD.

Schimmang, T., F. van der Hoeven, and U. Ruther. 1993. Gli3 expression is affected in the morphogenetic mouse mutants add and Xt. *Prog. Clin. Biol. Res.* **383:** 153–161.

Schimmang, T., M. Lemaistre, A. Vortkamp, and U. Ruther. 1992. Expression of the zinc finger gene Gli3 is affected in the morphogenetic mouse mutant extra-toes (Xt). *Development* **116:** 799–804.

Schimmang, T., S.I. Oda, and U. Ruther. 1994. The mouse mutant Polydactyly Nagoya (Pdn) defines a novel allele of the zinc finger gene Gli3. *Mamm. Genome* **5:** 384–386.

Shiroishi, T., T. Sagai, and K. Moriwaki. 1982. A new wild-derived H-2 haplotype enhancing K-IA recombination. *Nature* **300:** 370–372.

Shiroishi, T., T. Sagai, and K. Moriwaki. 1987a. Sexual preference of meiotic recombination within the H-2 complex. *Immunogenetics* **25:** 258–262.

Shiroishi, T., T. Sagai, S. Natsuume-Sakai, and K. Moriwaki. 1987b. Lethal deletion of the complement component C4 and steroid 21-hydroxylase genes in the mouse H-2 class III region, caused by meiotic recombination. *Proc. Natl. Acad. Sci.* **84:** 2819–2823.

Sweet, H.O. and P.W. Lane. 1980. X-linked polydactyly (Xpl) , a new mutation in the mouse. *J. Hered.* **71:** 207–209.

Tamura, K., Y. Aoki, and H. Ide. 1993. Induction of polarizing activity by retinoic acid occurs independently of duplicate formation in developing chick limb buds. *Dev. Biol.* **158:** 341–349.

Tickle, C. 1981. The number of polarizing region cells required to specify additional of digits in the developing chick wing. *Nature* **289:** 295–298.

Tickle, C.J., D. Summerbell, and L. Wolpert. 1975. Positional signalling and specification of digits in chick limb morphogenesis. *Nature* **254:** 199–202.

Tickle, C., B. Alberts, L. Wolpert, and J. Lee. 1982. Local application of retinoic acid to the limb bond [sic] mimics the action of the polarizing region. *Nature* **296:** 564–566.

Todt, W.L. and J.F. Fallon. 1987. Posterior apical ectodermal ridge removal in the chick wing bud triggers a series of events resulting in defective anterior pattern formation. *Development* **101:** 501–515.

Tsukurov, O., A. Boehmer, J. Flynn, J.-P. Nicolai, B.C.J. Ho, C. Tabin, J.G. Seideman, and C. Seidman. 1994. A complex bilateral polysyndactyly disease locus maps to chromosome 6. *Nature Genet.* **6:** 282–286.

Vortkamp, A., M. Gessler, and K.H. Grzeschik. 1991. GLI3 zinc-finger gene interrupted by translocations in Greig syndrome families. *Nature* **352:** 539–540.

Vortkamp, A., T. Franz, M. Gessler, and K.H. Grzeschik. 1992. Deletion of GLI3 supports the homology of the human Greig cephalopolysyndactyly syndrome (GCPS) and the mouse mutant extra toes (Xt). *Mamm. Genome* **3:** 461–463.

Wallin, J., J. Wilting, H. Koseki, R. Fistsh, B. Christ, and R. Balling. 1994. The role of *Pax-1* in axial skeleton development. *Development* **120:** 1109–1121.

Wanek, N., K. Muneoka, G. Holler-Dinsmore, R. Burton, and S.V. Bryant. 1989. A staging system for mouse limb development. *J. Exp. Zool.* **249:** 41–49.

Wanek, N., D.M. Gardiner, K. Muneoka, and S.V. Bryant. 1991. Conversion by retinoic acid of anterior cells into ZPA cells in the chick wing bud. *Nature* **350:** 81–83.

Wilkinson, D. G. 1992. Whole-mount in situ hybridization of vertebrate embryos. In *In situ hybridization: A practical approach* (ed. D. G. Wilknson), pp. 75–83. Oxford University Press, Oxford, UK.

Yujnovsky, O., D. Ayala, A. Vincitorio, H. Viale, N. Sakati, and W.L. Nyhan. 1974. A syndrome of polydactyly-syndactyly and triphalangeal thumbs in three generations. *Clin. Genet.* **6:** 51–59.

A duplicated zone of polarizing activity in polydactylous mouse mutants.

H Masuya, T Sagai, S Wakana, et al.

Genes Dev. 1995, **9:**
Access the most recent version at doi:10.1101/gad.9.13.1645